
Article:
Giriunas, L., Li, F., Sich, M. orcid.org/0000-0003-4155-3958 et al. (9 more authors) (2018) Formation of a macroscopically occupied polariton state in a tunable open-access microcavity under resonant excitation. Journal of Applied Physics, 124 (2). 025703. ISSN 0021-8979

https://doi.org/10.1063/1.5019933

Formation of a macroscopicaly occupied polariton state in a tunable open-access microcavity under resonant excitation

L. Giriunas,[1] Feng Li,[2,1,a)] M. Sich,[1,b)] E. Cancellieri,[1,3] R. P. A. Emmanuele,[1] A. A. P. Trichet,[4] I. Farrer,[5] D. A. Ritchie,[5] J. M. Smith,[4] D. M. Whittaker,[1] M. S. Skolnick,[1] and D. N. Krizhanovskii[1]

[1)] *Department of Physics and Astronomy, The University of Sheffield, Sheffield, S3 7RH, United Kingdom*

[2)] *Key Laboratory for Physical Electronics and Devices of the Ministry of Education & Shaanxi Key Laboratory of Photonics Technology for Information, Xian Jiaotong University, Xian 710049, China*

[3)] *Physics Department, Lancaster University, Lancaster, LA1 4YB, United Kingdom*

[4)] *Department of Materials, University of Oxford, Oxford, OX1 3PH, United Kingdom*

[5)] *Cavendish Laboratory, University of Cambridge, Cambridge, CB3 0HE, United Kingdom*

(Dated: 12 July 2018)

We experimentally demonstrate the formation of a macroscopically occupied state (condensation) of exciton-polaritons in a tunable 3D open-access microcavity system under resonant excitation. We observe a high conversion efficiency of polaritons from the pumped state to the ground mode, leading to population of the condensate 1.5 times greater than that of the driven state for a total number of polaritons of ∼110. Comparative numerical simulations show that coherent polariton-polariton scattering mechanisms alone cannot explain the observed experimental results and that other relaxation channels play an important role.

I. INTRODUCTION

Microcavity exciton-polaritons are quasi-particles arising from the strong coupling between the photonic mode of a microcavity and quantum well excitons embedded inside the cavity. Thanks to their excitonic part, Kerr-like optical nonlinearity in the polariton system is one of the highest observed in optics[1]. A very wide variety of effects arising from nonlinear polariton interactions have been observed, such as Bose-Einstein condensation, superfluidity[2–6], polariton optical parametric oscillation (OPO)[7–10], dark and bright solitons[11,12] and polaritonic topological singularities, such as vortices[13–15].

Both resonantly and non-resonantly excited polariton condensates have been thoroughly investigated in planar 2D structures (see *e.g.* Ref. 16). In microcavities with a strong 3D confinement, such as etched micropillars, polariton condensation and lasing under nonresonant excitation[17], and polariton OPO under resonant excitation[18] have been also studied. In these systems, with 3D confinement, polariton nonlinearities are expected to occur at very low total polariton populations due to strong polariton lateral confinement, making these systems essentially mesoscopic and potentially sensitive to quantum fluctuations[19,20]. Recently, a so-called 'open microcavity' system has been developed to provide strong optical confinement without the need for etching into the active region of quantum well (QW) excitons[21–23], hence preventing polariton losses from surface recombination effects. This cavity structure, consisting of one planar and one concave mirror with an air gap in between, provides strong lateral confinement down to sub-micron scale. The open microcavity system with (In)GaAs quantum wells as an active region has been used to observe strong exciton-photon coupling and polariton condensation under nonresonant excitation[22,24].

In this article, we report highly-efficient polariton relaxation and formation of a polariton macroscopically occupied state (MOS) under resonant excitation in the open microcavity system. We pump the first excited lower polariton state with a CW resonant laser, and above a certain threshold power we observe formation of a polariton MOS in the ground mode with a population 1.5 times greater than that of the pumped state, very significantly larger than the previously reported $0.01 - 0.02$ using pulsed excitation[25] in a planar microcavity. Formation of the polariton MOS is accompanied by bistable behaviour in the intensity dependence of both condensate and pumped mode emission. We also perform numerical studies, which show that coherent polariton-polariton and polariton-exciton scattering processes alone cannot explain such high relaxation efficiency and formation of the polariton MOS. Therefore, other relaxation mechanisms such as polariton-phonon, polariton-electron scattering and exciton reservoir-mediated relaxation should be taken into account.

II. RESULTS

We perform our experiments in transmission geometry. In this configuration the resonant excitation beam is incident on one side of the cavity, and emission is detected from the other side, therefore avoiding saturation of detectors by the reflected excitation beam. Another advantage of this geometry is that it allows an accurate estimate of the polariton population in the resonantly pumped mode by simply measuring the intensity

[a)] Electronic mail: felix831204@xjtu.edu.cn
[b)] Electronic mail: m.sich@sheffield.ac.uk

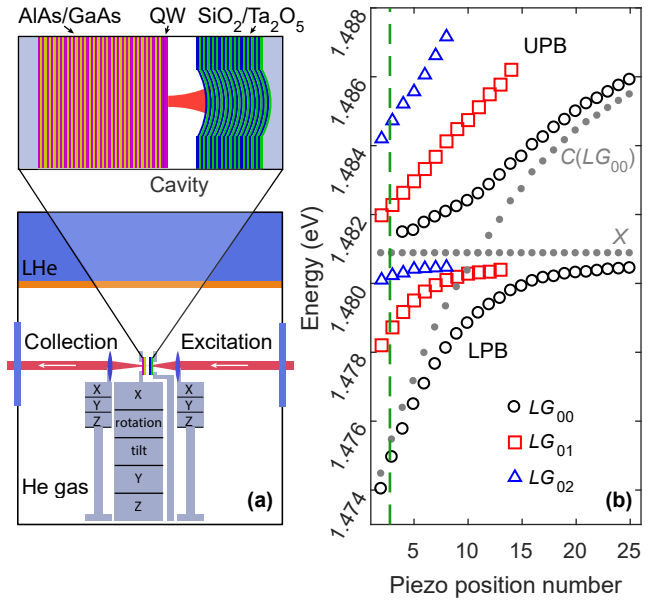

FIG. 1. (a) Schematic of the open microcavity structure and of the experimental setup. (b) Mode energies (detected in horizontal polarisation) as a function of piezo position. Anti-crossing is observed for lower polariton branches (LPB) associated with LG_{00} (black open circles), LG_{01} (red open squares) and LG_{02} (blue open triangles).The bare exciton, X, and cavity, $C(LG_{00})$, modes for the LG_{00} mode are shown in grey dotted lines.

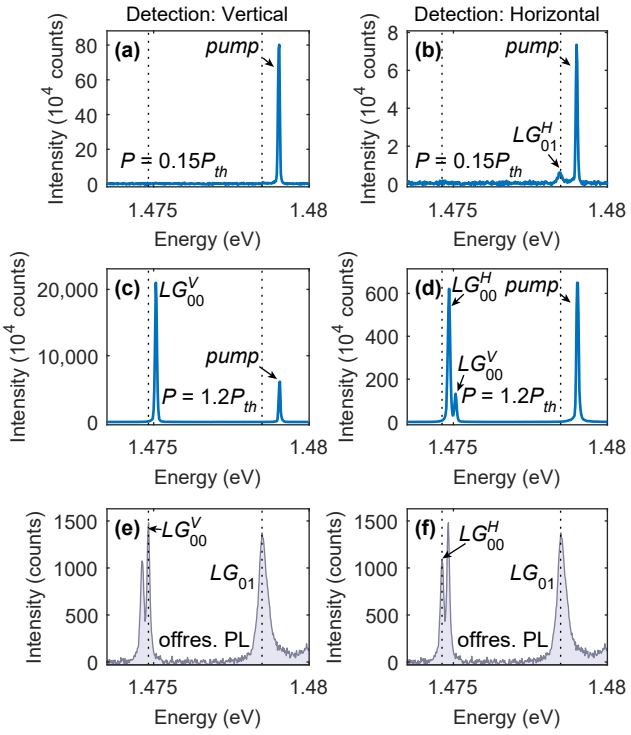

FIG. 2. Left column – spectra detected in vertical polarisation; right column – spectra detected in horizontal polarisation. Polarisation of the pump is vertical for all panels. (a), (b) Low excitation power, $P = 0.15P_{th}$. (c), (d) High excitation power, above the threshold, $P = 1.2P_{th}$. As a reference, panels (e) and (f) show polariton PL emission spectra recorded in both polarisations for the same exciton-photon detuning under off-resonant low power excitation. By comparing panels (e) and (c) and (a), (f) and (d) and (b) one can observe the blueshift of LG_{00} mode above threshold. The position of the pump, blueshifted with respect to the unperturbed LG_{01} polariton resonance, is also seen.

of the transmitted pump beam. Our microcavity consists of two mirrors: a planar 'bottom' semiconductor DBR (distributed Bragg reflector) mirror made of 27 pairs of AlAs/GaAs layers grown by molecular beam epitaxy, and a 'top' dielectric mirror – a 15-pair SiO_2/Ta_2O_5 DBR deposited on a concave surface fabricated using focused ion beam milling[21]. The Q-factor of the microcavity polariton mode measured at negative photon-exciton detuning (~ -8 meV) is about 15,000 and probably limited by the resolution of our setup. The concave mirror has a circular shape with a radius of curvature of 20 µm. The two mirrors together create a 3D-microcavity with discrete energy modes[22], which have lateral size (FWHM) in real space $\sim 1-2$ µm. A GaAs active region of $3\lambda/2$, with a single 10-nm $In_{0.04}Ga_{0.96}As$ QW embedded at the expected electric field antinode, is grown on top of the semiconductor mirror, as illustrated in Fig. 1(a). The two mirrors of the cavity are mounted vertically on individual stages with nanopositioners controlling their relative position and angle, as illustrated in Fig. 1(a). Two lenses (7.5 mm focal length, NA = 0.32), controlled by nanopositioners, are located at each side of the open cavity for excitation and collection. The entire setup is mounted in a helium exchange gas chamber, where the sample is cooled to 5 K, with optical windows at both sides.

To characterise the microcavity sample we applied continuous wave off-resonant excitation (red laser with 635 nm wavelength) and recorded photoluminescence (PL) spectra. We can control energy of the cavity modes by changing the distance between the 'top' and 'bottom' mirrors by moving the nanopositioner controlling the semiconductor 'bottom' mirror. In this way we scanned the cavity modes through the QW exciton energy ($E_X \simeq 1.481$ eV) and observed the anti-crossing behaviour between the cavity and exciton states characteristic of strong exciton-photon coupling[22]. We observed different modes of the Laguerre-Gaussian (LG) type, including LG_{00}, LG_{01}, and LG_{02}, as shown in Fig. 1(b). The derived vacuum Rabi splitting is $\hbar\Omega_R \simeq 3.46$ meV.

To perform the experiment, first, we set the cavity length such that the cavity-exciton detuning was $\delta_{LG_{01}} = -0.23$ meV for the LG_{01} mode and $\delta_{LG_{00}} = -5.52$ meV for the LG_{00} mode; this position is labelled by a green dashed line in Fig. 1(b). At these detunings both LG_{00} and LG_{01} are split into orthogonally linearly (H and V) polarised modes due to birefringence present probably in the top dielectric mirror, which has a slightly ellip-

tical shape. A polarisation splitting of $\simeq 0.22$ meV of the LG_{00} mode is observed. Then, we applied a linearly (V) polarised CW 'pump' laser with energy blue-detuned with respect to that of the higher energy V-polarised LG_{01} mode by $\simeq 0.4$ meV. We recorded spectra in H and V polarisations while changing the power of the pump laser: first increasing the power to the maximum (280 mW) and then decreasing back to the minimum value (5 mW). At low power, the transmitted pump laser dominates the emission spectra (Figs. 2(a,b)) with the H-polarised component being 10 times weaker than the V-polarised component. We also observe a weak photoluminescence emission from the LG_{01} H-polarised mode at energy 0.6 meV below that of the transmitted pump (Fig. 2b), whereas no emission is detected from the LG_{00} mode.

The real space integrated intensities of the LG_{00} mode emission and of the transmitted pump (labelled as LG_{00}^V, LG_{00}^H and pump) as a function of pump power are shown in Figs. 3(a,b) for V and H polarisations, respectively. At pump powers below 200 mW the intensity of the transmitted pump shows a nearly linear increase with power in both polarisations, and at the same time, the emission from the LG_{00} mode remains below or close to the noise level of the CCD detector. Because the pump laser is blue detuned with respect to the pump mode, the internal polariton field of the pump mode and hence the pump transmission intensity are expected to exhibit bistable behaviour with pump power due to repulsive polariton Kerr-like nonlinearity[26]. When the pump power is increased above $230-240$ mW energy of both the LG_{01}^H and LG_{01}^V modes shift upwards to the resonance with the pump laser leading to an abrupt increase of the pump transmission intensity (and hence the coherent populations of the pump V and H modes) in both polarisations. This transition is also accompanied by a strong increase of the emission intensities of the H and V-polarised LG_{00} modes (Figs. 3(a,b)), which become comparable to that of the pump mode in the corresponding polarisations (see Figs. 2(c,d)). At high power the blueshift of the LG_{00} mode is $\Delta E \simeq 220$ μeV, still $\simeq 200$ μeV below that of the uncoupled photonic mode. This, as well as the fact that the energy of the driving field is ~ 1.5 meV below the uncoupled LG_{01} cavity mode, ensures that the strong exciton-photon coupling is maintained in the system at high power.

With decreasing pump power hysteresis in the intensities of the pump transmission and LG_{00} mode emission is observed, characteristic of the optical polariton bistability. While sharing the same thresholds with the pump mode, the ground LG_{00} mode shows much stronger nonlinear increase of intensity (4 orders of magnitude), highlighting the nonlinear enhancement of the polariton relaxation rate to the ground state above the threshold when the pump mode becomes highly populated. More precisely the ratio of the LG_{00} to pump polariton populations is given by:

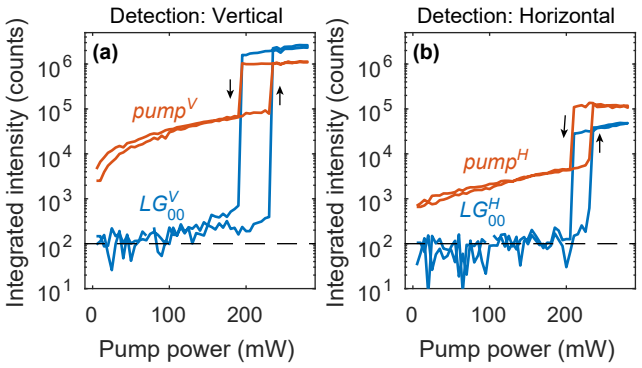

FIG. 3. Integrated intensity of LG_{00} and pump modes as a function of pump power in vertical (a) and horizontal (b) polarisations of detection. Dashed lines indicate noise level. Arrows indicate direction of the change of the pump power within the bistability hysteresis loop: increasing or decreasing.

$$\eta = \frac{\frac{I_{LG_{00}^V} + I_{LG_{00}^H}}{|C_{LG_{00}}|^2}}{\frac{I_{\mathrm{pump}^V} + I_{\mathrm{pump}^H}}{|C_{\mathrm{pump}}|^2}}$$

where $I_{LG_{00}^{V/H}/\mathrm{pump}^{V/H}}$ are integrated intensities of the LG_{00}/pump modes detected in vertical/horizontal linear polarisations; $C_{LG_{00}/\mathrm{pump}}$ are the photonic Hopfield coefficients of the LG_{00}/pump modes respectively. The data extracted from Fig. 3 yields the ratio between the ground LG_{00} and the pump modes $\eta \simeq 1.5$, when the pump is above the threshold.

The total combined output power of the LG_{00} PL emission and the transmitted pump intensity is measured to be $\simeq 1$ μW at maximum pump power, corresponding to an estimated total polariton number of $N \simeq 110$. Note that while both H- and V-polarised LG_{00} eigen-modes show nonlinear threshold behaviour, above the threshold the V-polarised LG_{00}^V mode is $\simeq 60$ times brighter than H-polarised LG_{00}^H mode. This means that the LG_{00}^V mode is macroscopically occupied with $\simeq 60-70$ particles, but LG_{00}^H mode contains on average only $1-2$ polaritons.

Assuming there are only interactions between polaritons residing in the pump (with polariton number $N_{\mathrm{pump}} = 40$) and the ground mode (with polariton number $N_{LG_{00}} = 70$), the expected energy blueshift of the pump mode ΔE_0, can be estimated as follows:

$$\Delta E_0 = \frac{1}{s} g_{XX} \left|X_{LG_{00}}\right|^2 \left|X_{\mathrm{pump}}\right|^2 N_{LG_{00}} + \\ + \frac{1}{s} g_{XX} \left|X_{\mathrm{pump}}\right|^4 N_{\mathrm{pump}} \simeq 37\ \mu\mathrm{eV},$$

where the exciton-exciton interaction constant is chosen to be[27] $g_{XX} = 10\ \mu\mathrm{eV} \cdot \mu\mathrm{m}^{-2}$, $s = 3\ \mu\mathrm{m}^2$ is mode area,

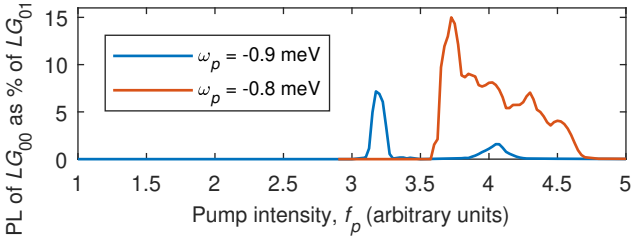

FIG. 4. Percentage of photon emission at the LG_{00} energy with respect to the emission at the pump (LG_{01}) energy as a function of the pump intensity f_p. The two curves correspond to two different frequencies for the quasi-resonant continuous-wave pump, ω_p.

and we estimate excitonic fractions of the ground and pump modes to be $|X_{LG_{00}}|^2 = 0.13$ and $|X_{\rm pump}|^2 = 0.43$ respectively. The estimated value of the blueshift of the pump mode is much smaller than the experimental value of $\simeq 0.4$ meV, indicating that there is also an interaction between LG_{00} and pump (LG_{01}) polariton modes and highly populated exciton-reservoir states (localised excitons, dark excitons and high-energy high-momenta excitons) significantly contributing to the observed energy shift[1].

There are several mechanisms which may lead to transfer of polaritons from the driven to the ground mode in this system. Firstly, a coherent four-wave mixing process, where two polaritons from the pump state scatter to the 'signal' LG_{00} state and the 'idler' state such that $2E_{\rm pump} = E_{LG_{00}} + E_i$ associated with the upper polariton branches, which become macroscopically populated and form an 'optical parametric oscillator' (OPO). This mechanism has been extensively studied in planar microcavities[7–10]. We did not observe any idler emission at energy E_i, which in our case would be very close to the QW exciton energy, E_X, where polariton PL emission is naturally very weak (expected to be ~ 2 orders of magnitude smaller than the signal) since it is dominated by the excitonic component. Secondly, even though the energy of the pump mode is below that of the bare exciton, coherent polariton-polariton scattering may still occur from the pump to higher energy high-momenta excitons with high density of states due to the finite exciton linewidth (~ 1 meV). From exciton states polaritons may further relax down to the ground state via coherent exciton-exciton interactions[28,29]. Finally, other relaxation mechanisms may involve polariton-phonon and polariton-electron scattering[30] as well as relaxation through reservoir of localised or dark exciton states, when polaritons completely decohere with respect to the excited mode[31].

To determine whether coherent polariton-polariton and polariton-exciton interactions alone can explain the observed experimental results or other incoherent processes should be considered we performed theoretical studies, where we took into account only coherent interparticle interactions. We model the open cavity system with a generalized Gross-Pitaevskii equation[32,33] (GP) for coupled cavity exciton fields (ψ_C and ψ_X) and include the effect of decay and resonant pumping ($\hbar = 1$):

$$\partial_t \begin{pmatrix} \psi_X \\ \psi_C \end{pmatrix} = \left[H_0 + \begin{pmatrix} g_X|\psi_X|^2 & 0 \\ 0 & V_C \end{pmatrix} \right] \begin{pmatrix} \psi_X \\ \psi_C \end{pmatrix} + \begin{pmatrix} 0 \\ F \end{pmatrix},$$

where the term H_0 is the single particle Hamiltonian:

$$\begin{pmatrix} \omega_X(-i\nabla) - i\kappa_X/2 & \Omega_R/2 \\ \Omega_R/2 & \omega_C(-i\nabla) - i\kappa_c/2 \end{pmatrix},$$

and $\omega_C(-i\nabla) = \omega_C^0 - \nabla^2/2m_c$ is the cavity dispersion with a photon mass $m_C = 2.3\times10^{-5} m_0$, where m_0 is the bare electron mass. For our simulations we fix to zero the flat exciton dispersion $\omega_X(-i\nabla) = \omega_X^0 = 0$, and set the exciton photon detuning $\delta_{X-ph} = \omega_X^0 - \omega_C^0 = -11$ meV. The parameters $\Omega_R = 3.50$ meV, $\kappa_X = 0.20$ meV, and $\kappa_C = 0.05$ meV are the Rabi frequency and the exciton and photon decay rates. To simulate the injection of polaritons we use a continuous-wave quasi-resonant pump with a Gaussian shape $F = f_p e^{-i\omega_p t - (r-r_0)^2/2\sigma_p^2}$, where f_p is pump intensity, ω_p is pump frequency relative to LG_{01} bare cavity mode which varies from -0.9 to -0.8 meV, $r_0 = 0.5$ µm represents a slight mismatch between centres of the potential and pump enabling coupling of the Gaussian pump beam to the LG_{01} polariton mode, and $\sigma_p = 2.5$ µm. Finally, in order to simulate the curvature of the top mirror, we introduce a harmonic confinement of the photonic component: $V_C = \frac{1}{2} m_C \omega_{hp}^2 r^2$, where $\omega_{hp} = 5.0$ meV is the strength of the harmonic confinement. The exciton repulsive interaction strength $g_X = 1$ is set to one by rescaling the fields and the pump strengths. Overall, the model parameters were chosen in such a way that the confined polariton energies and the excitation conditions match closely those in the experiment. Finally, we use a Runge-Kutta algorithm (see *e.g.* Ref. 34) to simulate the dynamics of the GP equation. We start from an empty system, turn on the pump and reach a steady state situation. At this point we evaluate the spectra of the emitted light and derive the ratio between the population at the LG_{00} energy and the population at the pump energy. The photonic efficiency shown in Fig. 4 correspond to an even smaller overall efficiency since the LG_{00} mode is more photonic than the pump mode. The highest simulated conversion efficiency is only on the order of $10-15\%$ for the photonic component, which is significantly less than the experimental value. The origin of the switching 'off' of the OPO after the peak at 3.3 a.u. and subsequent switching 'on' at 3.8 a.u. can be attributed to the interplay between higher-order scattering processes and the spatial dependence of the different modes. Since the modes and the pump are not homogeneous in space, different parts in different spatial points can reach the optimal OPO phase matching conditions at different pump powers. Therefore, we confirm that coherent interparticle

scatterings alone cannot explain such a high conversion efficiency from the pumped to the ground mode observed in the experiment. Absorption of the pumped polaritons due to other scattering mechanisms and relaxation channels mentioned above together with the 3D confinement may play a significant role in achieving such a high efficiency. We note, that in our experiment it is not possible to reliably estimate the population of exciton reservoir states and hence provide a conversion efficiency from the absorbed polaritons to signal, as was done for OPO experiments in planar microcavities, *e.g.* Ref. 35. It is not clear why under pulsed resonant excitation the conversion efficiency from pump to signal state is deduced to be only $0.01 - 0.02$[25], much smaller than in our CW experiment. Probably, CW excitation allows more efficient population of incoherent exciton reservoir[1], the lifetime of which can be in nanosecond time scales.

Finally, we note that incoherent polariton relaxation is expected to depolarise polaritons. In our experiment, we observe that the MOS is always V-polarised for either H- or V-polarised pump, probably because LG_{00}^{V} is closer in energy to the exciton level and hence experiences a higher gain and/or this mode has lower photonic losses than the LG_{00}^{H} state.

III. DISCUSSION

In conclusion, we have demonstrated formation of a polariton macroscopically occupied state in the ground confined lower polariton mode, LG_{00}, in a 3D microcavity under resonant excitation of the 1-st excited transverse polariton mode, LG_{01}. Population of the MOS exceeds that of the driven state by 1.5 times and the total polariton population is $\simeq 100$. Numerical modelling and estimation of the polariton interaction strength indicates that relaxation through the incoherent exciton reservoir state also very likely takes place. Such small and efficient 3D microcavities are promising for applications in integrated photonic circuits and, potentially, in quantum polaritonics. Even though the conversion efficiency is high when considering the polaritons inside the cavity, the coupling of the external pumping laser into the cavity is not yet an efficient process, which could be improved by matching the spatial profiles of the pumping laser to the LG_{01} mode of the cavity using, for example, a spatial light modulator.

MS and DNK acknowledge the support from the Leverhulme Trust grant No. RPG-2013-339. LG, FL, MS, EC, RPAE, MSS and DNK acknowledge the support from the EPSRC grants EP/J007544/1, EP/N031776/1, and the ERC Advanced Grant EXCIPOL 320570.

[1] P. M. Walker, L. Tinkler, B. Royall, D. V. Skryabin, I. Farrer, D. A. Ritchie, M. S. Skolnick, and D. N. Krizhanovskii, Phys. Rev. Lett. **119**, 097403 (2017).
[2] J. Kasprzak, M. Richard, S. Kundermann, A. Baas, P. Jeambrun, J. M. J. Keeling, F. M. Marchetti, M. H. Szymanska, R. Andre, J. L. Staehli, V. Savona, P. B. Littlewood, B. Deveaud, and L. S. Dang, Nature **443**, 409 (2006).
[3] A. Amo, J. Lefrere, S. Pigeon, C. Adrados, C. Ciuti, L. Carusotto, R. Houdre, E. Giacobino, and A. Bramati, Nature Physics **5**, 805 (2009).
[4] I. Carusotto and C. Ciuti, Reviews of Modern Physics **85**, 299 (2013).
[5] H. Deng, H. Haug, and Y. Yamamoto, Reviews of Modern Physics **82**, 1489 (2010).
[6] D. Sanvitto and S. Kéna-Cohen, Nature Materials **15**, 1061 (2016).
[7] P. G. Savvidis, J. J. Baumberg, R. M. Stevenson, M. S. Skolnick, D. M. Whittaker, and J. S. Roberts, Physical Review Letters **84**, 1547 (2000).
[8] R. M. Stevenson, V. N. Astratov, M. S. Skolnick, D. M. Whittaker, M. Emam-Ismail, A. I. Tartakovskii, P. G. Savvidis, J. J. Baumberg, and J. S. Roberts, Physical Review Letters **85**, 3680 (2000).
[9] C. Ciuti, P. Schwendimann, and A. Quattropani, Physical Review B **63**, 041303 (2001).
[10] D. Bajoni, E. Peter, P. Senellart, J. L. Smirr, I. Sagnes, A. Lematre, and J. Bloch, Applied Physics Letters **90**, 051107 (2007).
[11] A. Amo, S. Pigeon, D. Sanvitto, V. G. Sala, R. Hivet, I. Carusotto, F. Pisanello, G. Leménager, R. Houdré, E. Giacobino, C. Ciuti, and A. Bramati, Science **332**, 1167 (2011).
[12] M. Sich, D. N. Krizhanovskii, M. S. Skolnick, A. V. Gorbach, HartleyR, D. V. Skryabin, E. A. Cerda-Mendez, BiermannK, R. Hey, and P. V. Santos, Nature Photonics **6**, 50 (2012).
[13] K. G. Lagoudakis, M. Wouters, M. Richard, A. Baas, I. Carusotto, R. Andre, L. S. Dang, and B. Deveaud-Pledran, Nat Phys **4**, 706 (2008).
[14] G. Nardin, G. Grosso, Y. Léger, B. Pitka, F. Morier-Genoud, and B. Deveaud-Plédran, Nature Physics **7**, 635 (2011).
[15] T. Boulier, E. Cancellieri, N. D. Sangouard, Q. Glorieux, A. V. Kavokin, D. M. Whittaker, E. Giacobino, and A. Bramati, Phys. Rev. Lett. **116**, 116402 (2016).
[16] N. P. Proukakis, D. W. Snoke, and P. B. Littlewood, eds., Universal Themes of Bose-Einstein Condensation (Cambridge University Press, 2017).
[17] L. Ferrier, E. Wertz, R. Johne, D. Solnyshkov, P. Senellart, I. Sagnes, A. Lemaître, G. Malpuech, and J. Bloch, Physical Review Letters **106**, 126401 (2011).
[18] L. Ferrier, S. Pigeon, E. Wertz, M. Bamba, P. Senellart, I. Sagnes, A. Lemàtre, C. Ciuti, and J. Bloch, Applied Physics Letters **97**, 2 (2010).
[19] T. Fink, A. Schade, S. Höfling, C. Schneider, and A. Imamoglu, Nature Physics **14**, 365 (2018).
[20] M. Calvanese Strinati, E. Cornfeld, D. Rossini, S. Barbarino, M. Dalmonte, R. Fazio, E. Sela, and L. Mazza, Phys. Rev. X **7**, 021033 (2017).
[21] P. R. Dolan, G. M. Hughes, F. Grazioso, B. R. Patton, and J. M. Smith, Optics Letters **35**, 3556 (2010).
[22] S. Dufferwiel, F. Fras, A. Trichet, P. M. Walker, F. Li, L. Giriunas, M. N. Makhonin, L. R. Wilson, J. M. Smith, E. Clarke, M. S. Skolnick, and D. N. Krizhanovskii, Applied Physics Letters **104**, (2014).
[23] B. Besga, C. Vaneph, J. Reichel, J. Estève, A. Reinhard, J. Miguel-Sánchez, A. Imamolu, and T. Volz, Physical Review Applied **3**, 014008 (2015).
[24] S. Dufferwiel, F. Li, E. Cancellieri, L. Giriunas, A. A. P. Trichet, D. M. Whittaker, P. M. Walker, F. Fras, E. Clarke, J. M. Smith, M. S. Skolnick, and D. N. Krizhanovskii, Physical Review Letters **115**, 246401 (2015).
[25] A. A. Demenev, A. A. Shchekin, A. V. Larionov, S. S. Gavrilov, V. D. Kulakovskii, N. A. Gippius, and S. G. Tikhodeev, Phys. Rev. Lett. **101**, 136401 (2008).
[26] A. Baas, J. P. Karr, M. Romanelli, A. Bramati, and E. Giacobino, Physical Review B **70**, 161307 (2004).
[27] P. M. Walker, L. Tinkler, D. V. Skryabin, A. Yulin, B. Royall, I. Farrer, D. A. Ritchie, M. S. Skolnick, and D. N. Krizhanovskii, Nature Communications **6**, 8317 (2015).
[28] D. Krizhanovskii, A. Tartakovskii, A. Chernenko, V. Kulakovskii,

M. Emam-Ismail, M. Skolnick, and J. Roberts, Solid State Communications **118**, 583 (2001).
[29] P. G. Savvidis, J. J. Baumberg, D. Porras, D. M. Whittaker, M. S. Skolnick, and J. S. Roberts, Phys. Rev. B **65**, 073309 (2002).
[30] A. I. Tartakovskii, D. N. Krizhanovskii, G. Malpuech, M. Emam-Ismail, A. V. Chernenko, A. V. Kavokin, V. D. Kulakovskii, M. S. Skolnick, and J. S. Roberts, Phys. Rev. B **67**, 165302 (2003).
[31] D. Krizhanovskii, G. Dasbach, A. Dremin, V. Kulakovskii, N. Gippius, M. Bayer, and A. Forchel, Solid State Communications **119**, 435 (2001).
[32] E. Cancellieri, F. M. Marchetti, M. H. Szymańska, and C. Tejedor, Phys. Rev. B **83**, 214507 (2011).
[33] E. Cancellieri, J. K. Chana, M. Sich, D. N. Krizhanovskii, M. S. Skolnick, and D. M. Whittaker, Phys. Rev. B **92**, 174528 (2015).
[34] W. H. Press, S. A. Teukolsky, W. T. Vetterling, and B. P. Flannery, Numerical Recipes: The Art of Scientific Computing, 3rd ed. (Cambridge University Press, 2007) p. 1235.
[35] J. J. Baumberg, P. G. Savvidis, R. M. Stevenson, A. I. Tartakovskii, M. S. Skolnick, D. M. Whittaker, and J. S. Roberts, Phys. Rev. B **62**, R16247 (2000).